Rational Synthesis of Metalla–Sulphur–Nitrogen Complexes: Use of $[Me_2SnS_2N_2]_2$ in the Preparation of Complexes of the Type $[M(S_2N_2H)(PR_3)_2]X$ (M = Pt or Pd). *X*-Ray Structures of $[Pt(S_2N_2H)(PEt_3)_2][Me_2SnCl_3]$, $[Pt(S_2N_2H)(PBu^n_3)_2]_2[PF_6]Cl$, and $[\{Co(S_2N_2H)_2\}_2\{Ph_2P(O)CH_2CH_2P(O)Ph_2\}]$†

Ray Jones, Christopher P. Warrens, David J. Williams, and J. Derek Woollins *
Department of Chemistry, Imperial College of Science and Technology, South Kensington, London SW7 2AY

Reaction of $(Me_2SnS_2N_2)_2$ with *cis*-$[MCl_2(PR_3)_2]$ (M = Pt, PR_3 = PMe_3, PEt_3, PPr^n_3, PBu^n_3, PMe_2Ph, $PMePh_2$, PPh_3, or $\frac{1}{2}Ph_2PCH_2CH_2PPh_2$; M = Pd, PR_3 = $\frac{1}{2}Ph_2PCH_2CH_2PPh_2$) in dichloromethane yields $[M(S_2N_2H)(PR_3)_2][Me_2SnCl_3]$. If the reaction is carried out in the presence of $[NH_4][PF_6]$ then PF_6^- salts are obtained. The complexes have been characterised by microanalysis, i.r., ^{31}P and ^1H n.m.r., and, in the case of $[Pt(S_2N_2H)(PEt_3)_2][Me_2SnCl_3]$ and $[Pt(S_2N_2H)(PBu^n_3)_2]_2[PF_6]Cl$, by *X*-ray crystallography. The reaction of $[CoCl_2\{Ph_2P(O)CH_2CH_2P(O)Ph_2\}]$ with $(Me_2SnS_2N_2)_2$ gave $[\{Co(S_2N_2H)_2\}_2\{Ph_2P(O)CH_2CH_2P(O)Ph_2\}]$, whose structure was established by *X*-ray crystallography.

Compounds containing the $S_2N_2H^-$ ligand have been known for a number of years[1-3] but there are no reported examples of mixed-ligand complexes containing phosphine ligands, although compounds of the type $[M(S_2N_2)(PR_3)_2]$ (M = Pd or Pt, R = alkyl or aryl) are known.[4] These latter compounds were prepared by reaction of *cis*-$[MCl_2(PR_3)_2]$ with $Na(S_3N_3)$ whilst the majority of complexes containing $S_2N_2^{2-}$ or $S_2N_2H^-$ are obtained from reactions involving tetrasulphur tetranitride, S_4N_4. We are currently investigating routes to metal–sulphur–nitrogen complexes and are particularly interested in developing rational syntheses. For example, deprotonation of S_7NH (at −78 °C) provides[5] an *in situ* source of S_3N^- which may be used in the formation of $[AuCl_2(S_3N)]$, whilst reaction of $(Me_3SiN)_2S$ with $[Pt(C_2H_4)(PPh_3)_2]$ gives $[Pt(NSNSiMe_3)_2(PPh_3)_2]$.[6] This latter reaction is a rare example of the use of a silyl reagent in the formation of a metal–sulphur–nitrogen complex and its success prompted us to consider the use of other Group 4 reagents in a similar fashion. We report here that reaction of $(Me_2SnS_2N_2)_2$[7] with *cis*-$[MCl_2(PR_3)_2]$ in dichloromethane provides a useful and rational route to complexes of the type $[M(S_2N_2H)(PR_3)_2][X]$ (X = Me_2SnCl_3, PF_6, or BF_4).[2-14] The *X*-ray structures of two examples of these compounds (M = Pt; PR_3 = PMe_3, X = PF_6; PR_3 = PMe_2Ph, X = BF_4) were the subject of a preliminary communication[8] and are of particular interest since they reveal stacked columns of cations and anions. The structures of two more examples of this class of compounds are reported and compared with the previous two herein.

Experimental

All manipulations were performed under an inert atmosphere (Ar or N_2). Solvents were dried before use: CH_2Cl_2 was distilled from CaH_2 and stored over 4 Å molecular sieves; diethyl ether, tetrahydrofuran (thf), and n-hexane were distilled from sodium–benzophenone. The ^{31}P-$\{^1H\}$ and ^1H n.m.r. spectra were recorded using a JEOL FX90Q spectrometer operating at 36.21 and 89.55 MHz and are referred to external 85% H_3PO_4 and internal $SiMe_4$ respectively. Infrared spectra were obtained from KBr discs using a Perkin-Elmer 683 spectrophotometer. E.s.r. spectra were obtained using a Varian E9 instrument. Elemental analyses were performed by Pascher Microanalytical (Germany) and by the departmental microanalytical service. Chloride and PF_6^- levels in the final complexes were established using a Dionex ion chromatograph.

The compounds $(Me_2SnS_2N_2)_2$,[7] $[MCl_2(dppe)]$ [dppe = 1,2-bis(diphenylphosphino)ethane; M = Pt,[9] M = Pd[10]], and *cis*-$[PtCl_2(PPh_3)_2]$[11] were prepared by standard methods. The complexes *cis*-$[PtCl_2(PR_3)_2]$ (PR_3 = PMe_3, PMe_2Ph, $PMePh_2$, PEt_3, PPr^n_3, or PBu^n_3) were prepared from $[PtCl_2(cod)]$ (cod = cyclo-octa-1,5-diene)[12] and a stoicheiometric quantity of the phosphine and recrystallised from CH_2Cl_2–Et_2O.

Preparation of [1,2-*Bis*(*diphenylphosphoryl*)*ethane*]*dichlorocobalt*(II).—This was obtained from the reaction reported[13] to give $[CoCl_2(dppe)]$. $CoCl_2 \cdot 6H_2O$ (0.62 g, 2.6 mmol) and dppe (1.0 g, 2.5 mmol) were mixed in acetone (125 cm^3) in air and allowed to stand for 3 weeks. The initially green solution deposited green crystals of $[\{CoCl(dppe)\}_2]$ (0.42 g); these were filtered off and after a further 2 d the solution became blue and contained crystals of the blue product. These were filtered off, washed with n-hexane (20 cm^3), and dried *in vacuo*. Yield 0.76 g, 71% (Found: C, 56.0; H, 4.50. $C_{26}H_{24}Cl_2CoO_2P_2$ requires C, 55.75; H, 4.30%). I.r. (cm^{-1}): 3 040w, 2 905w, 1 683m, 1 587w, 1 480m, 1 432s, 1 408m, 1 148br s, 1 120s, 1 094s, 1 067s, 1 023w, 993m, 723s, 688s, 553s, 538s, 502s, 335m, and 305m.

Reaction of $[CoCl_2(dppoe)]$ *with* $(Me_2SnS_2N_2)_2$.—$[CoCl_2(dppoe)]$ [dppoe = 1,2-bis(diphenylphosphoryl)ethane] (100 mg, 0.18 mmol) and $(Me_2SnS_2N_2)_2$ (**1**) (45.6 mg, 0.095 mmol) were stirred together in degassed CH_2Cl_2 (10 cm^3) for 20 h at room temperature. The dark green solid formed in this reaction was filtered off (and discarded) from the purple solution. The filtrate was evaporated to dryness under reduced pressure and the resulting mauve solid washed with n-hexane (2 × 10 cm^3) and then dried *in vacuo*. Crystals of $[\{Co(S_2N_2H)_2\}_2(dppoe)]$ (**15**) suitable for *X*-ray analysis were obtained by recry-

† [Di(azathien)-1-yl-S^1N^4]bis(triethylphosphine)platinum(II) trichlorodimethylstannate(IV), bis{[di(azathien)-1-yl-S^1N^4]bis(tri-n-butylphosphine)platinum(II)} chloride hexafluorophosphate, and [1,2-bis(diphenylphosphoryl)ethane]bis{bis[di(azathien)-1-yl-S^1N^4]cobalt(II)} respectively.

Supplementary data available: see Instructions for Authors, *J. Chem. Soc., Dalton Trans.*, 1987, Issue 1, pp. xvii—xx.

Table 1. Microanalytical data and melting points for the reported compounds

Compound	Colour	M.p./°C	Analysis[a] (%) C	H	N
(2) $[Pt(S_2N_2H)(PPh_3)_2][PF_6]$	Yellow-green	205—216[b]	44.55 (45.15)	3.45 (3.25)	2.65 (2.90)
(3) $[Pt(S_2N_2H)(PPh_3)_2][BF_4]$	Yellow	258—259[b]	47.05 (48.05)	3.45 (3.45)	2.90 (3.10)
(4) $[Pt(S_2N_2H)(PPh_3)_2][Me_2SnCl_3]$	Yellow	236—238[b]	43.2 (42.75)	3.65 (3.50)	2.25 (2.60)
(5) $[Pt(S_2N_2H)(PMePh_2)_2][PF_6]$	Lime green	123—125	37.45 (37.45)	3.25 (3.25)	3.25 (3.35)
(6) $[Pt(S_2N_2H)(PMePh_2)_2][Me_2SnCl_3]$	Yellow-green		35.1 (35.6)	3.40 (3.50)	2.90 (2.95)
(7) $[Pt(S_2N_2H)(PMe_2Ph)_2][PF_6]$	Lime green	224—226[b]	27.1 (27.1)	3.25 (3.25)	4.35 (3.95)
(8) $[Pt(S_2N_2H)(PMe_3)_2][PF_6]$	Lime green	199—200[b]	13.6 (12.3)	3.55 (3.25)	5.25 (4.80)
(9) $[Pt(S_2N_2H)(PEt_3)_2][PF_6]$	Green-yellow	154—156	20.9 (21.55)	4.50 (4.65)	3.90 (4.20)
(11) $[Pt(S_2N_2H)(PPr^n_3)_2][PF_6]$	Green	111—112	28.75 (28.7)	5.70 (5.75)	3.70 (3.70)
(12) $[Pt(S_2N_2H)(PBu^n_3)_2]_2[PF_6]Cl$	Green	133—135	35.75 (36.8)	7.00 (7.10)	3.50 (3.60)
(13) $[Pt(S_2N_2H)(dppe)][PF_6]$	Green	261—262[b]	37.75 (37.55)	3.00 (3.05)	3.15 (3.35)
(14) $[Pd(S_2N_2H)(dppe)][PF_6]$	Yellow	239—241[b]	42.0 (42.05)	3.30 (3.40)	3.70 (3.75)

[a] Calculated values given in parentheses. [b] With decomposition.

stallisation from CH_2Cl_2–n-hexane. Yield 30 mg, 18%. I.r. (cm^{-1}): 3 140br w, 3 040w, 2 905w, 1 585w, 1 478w, 1 431s, 1 405m, 1 255w, 1 151vbr s, 1 116s, 1 091s, 1 061w, 1 020w, 990w, 787m, 758m, 731s, 720s, 687s, 590m, 548s, 528s, 503s, 402m, and 339w. A dichloromethane solution of the deep purple crystals gave e.s.r. signals (frozen solution, −196 °C) of g = 4.23, 2.62, and 2.02 with hyperfine splitting on the last signal due to ^{59}Co of 26 mT, in good agreement with the literature for $[Co(S_2N_2H)_2]$.[2]

Preparation of $[Pt(S_2N_2H)(PEt_3)_2][Me_2SnCl_3]$ **(10)**.—$[PtCl_2(PEt_3)_2]$ (100 mg, 0.2 mmol) and **(1)** (48 mg, 0.1 mmol) were stirred together in degassed CH_2Cl_2 (10 cm^3) for 18 h. The resulting, slightly cloudy, yellow solution was filtered through Celite and the filtrate evaporated to dryness under reduced pressure. The resultant yellow solid was washed with diethyl ether (3 × 10 cm^3) and dried *in vacuo*. The dried material was dissolved in CH_2Cl_2 (*ca.* 2 cm^3) and diethyl ether (*ca.* 5 cm^3) added to give a turbid solution which on cooling to −20 °C gave crystals of the green–yellow *cis*-$[Pt(S_2N_2H)(PEt_3)_2][Me_2SnCl_3]$ suitable for *X*-ray analysis. Yield 55 mg, 45%.

Preparation of $[Pt(S_2N_2H)(PPh_3)_2][Me_2SnCl_3]$.—*cis*-$[PtCl_2(PPh_3)_2]$ (100 mg, 0.126 mmol) and **(1)** (30.5 mg, 0.063 mmol) were refluxed together in ethanol-free chloroform (10 cm^3) for 1 h. The resulting clear orange solution was evaporated to dryness. The yellow solid from this treatment was washed with diethyl ether (2 × 5 cm^3), extracted into dichloromethane (5 cm^3), filtered through Celite, and after reduction in volume *ca.* 2 cm^3 treated with diethyl ether (10 cm^3) and n-hexane (5 cm^3). Cooling to −20 °C gave the microcrystalline yellow product. Yield 55 mg, 41%.

Reaction of cis-$[MCl_2(PR_3)_2]$ (M = Pt, PR_3 = PMe_3, PEt_3, PPr^n_3, PBu^n_3, PMe_2Ph, $PMePh_2$, PPh_3 *or* ½dppe; M = Pd, PR_3 = ½dppe) *with* $(Me_2SnS_2N_2)_2$ *and* $[NH_4][PF_6]$. *Preparation of* $[M(S_2N_2H)(PR_3)_2][X]$ (X = BF_4 *or* PF_6).—All of these complexes (Table 1) were prepared by the same general method, illustrated here for $[Pt(S_2N_2H)(PPr^n_3)_2][PF_6]$. *cis*-$[PtCl_2(PPr^n_3)_2]$ (75 mg, 0.128 mmol), **(1)** (31 mg, 0.064 mmol), and $[NH_4][PF_6]$ (20.8 mg, 0.128 mmol) were stirred together in degassed CH_2Cl_2 (10 cm^3) for 2 h. The resulting solution was filtered, evaporated to dryness under reduced pressure, and the yellow-green solid that was obtained was washed with diethyl ether (2 × 10 cm^3) and dried *in vacuo*. Recrystallisation from CH_2Cl_2–Et_2O gave the final product except for that with PR_3 = PBu^n_3 which was obtained by crystallisation from diethyl ether at −20 °C. The same general method was also used to prepare BF_4^- salts, with ammonium tetrafluoroborate being used rather than the hexafluorophosphate. The complexes were obtained as air-stable, crystalline solids with yields in the range 40—50%.

Crystal Data.—$[Pt(S_2N_2H)(PEt_3)_2][Me_2SnCl_3]$ **(10)**. $C_{14}H_{37}Cl_3N_2P_2PtS_2Sn$, M = 779.64, monoclinic, a = 16.562(7), b = 16.147(5), c = 21.362(6) Å, β = 105.82(3)°, U = 5 496(3) $Å^3$, space group $A2/a$, Z = 8, D_c = 1.89 g cm^{-3}, μ(Cu-K_α) = 223.3 cm^{-1}, λ = 1.541 78 Å, F(000) = 2 992. Green, air-stable prisms, crystal dimensions 0.15 × 0.15 × 0.09 mm.

$[Pt(S_2N_2H)(PBu^n_3)_2]_2[PF_6]Cl$ **(12)**. $C_{48}H_{110}ClF_6N_4P_5Pt_2S_4$, M = 1 566.09, triclinic, a = 12.566(2), b = 14.309(3), c = 20.449(6) Å, α = 80.33(2), β = 79.54(2), γ = 82.67(2)°, U = 3 546(1) $Å^3$, space group $P\bar{1}$, Z = 2, D_c = 1.47 g cm^{-3}, μ(Cu-K_α) = 103 cm^{-1}, λ = 1.541 78 Å, F(000) = 1 584. Green, air-stable prisms, crystal dimensions 0.07 × 0.07 × 0.19 mm.

$[\{Co(S_2N_2H)_2\}_2(dppoe)]$ **(15)**. $C_{26}H_{28}Co_2N_8O_2P_2S_8$, M = 920.86, monoclinic, a = 12.054(4), b = 10.948(4), c = 14.920(9) Å, β = 108.67(4)°, U = 1 865(1) $Å^3$, space group $P2_1/n$, Z = 2, D_c = 1.65 g cm^{-3}, μ(Cu-K_α) = 126 cm^{-1}, λ = 1.541 78 Å, F(000) = 936. Violet-blue air-stable prisms, crystal dimensions 0.27 × 0.23 × 0.15 mm.

Data Collection and Processing.—Nicolet R3m diffractometer, ω-scan method (θ ≤ 50°),* graphite-monochromated Cu-K_α radiation. For **(10)**, **(12)**, and **(15)**: 2 175, 7 290, and 1 913 independent measured reflections; 2 015, 6 396, and 1 512 respectively considered observed [$|F_o|$] > 3σ($|F_o|$)], corrected for Lorentz and polarisation factors; Gaussian absorption correction (face indexed crystals).

Structure Analysis and Refinement.—All three structures were solved by direct methods and the non-hydrogen atoms refined anisotropically with the exception of the partial-occupancy carbon atoms [C(4A), C(4B); C(28A), C(28B)] in **(12)** (site occupation factors 0.6 and 0.4 respectively) which were refined isotropically. In all cases the NH hydrogen atom positions were determined from ΔF maps and these atoms were refined isotropically. In **(10)** and **(15)** the positions of all the other hydrogen atoms were idealised (C–H 0.96 Å), assigned isotropic thermal parameters, U(H) = 1.2$U_{eq.}$(C), and allowed to ride on

* Value of $\theta_{max.}$ chosen to give adequate ratio of observations to variable structure parameters.

Table 2. Infrared (and in some cases, Raman) absorptions (cm^{-1}) due to the $S_2N_2H^-$ ligand

Compound	ν(NH)	δ(NH)	ν(NS)	ν(NS)	ν(PF)	ν(NS)	δ(NH)	δ(PF)	ν(MN)	ν(MS)	δ(NS)
(2)	3 255w		1 052mw		840vs	708 (sh)		549s			350mw
(3)	3 230w		1 050 (sh)	870w				545s			347mw
(4)			1 047mw				614w				350mw
(5)	3 295vw		1 049m		840vs			560s			350mw
(7) I.r.	3 324w	1 220w	1 052m		840vs		615w	558s		358w	344mw
Raman		1 194br,w	1 063m	881w			618w			355w	341s
		1 100m									
(8)	3 665w	1 240br,w	1 054mw		840vs	712m(?)		561s	476m	374mw	337m
	3 585w										
(9)	3 315w	1 185w	1 044 (sh)		840vs	709mw	615w	560s	469w		344mw
(11)	3 310w		1 043 (sh)		840vs	708mw		560s			346mw
(12)	3 315w		1 050 (sh)		840vs	708mw		561s			347mw
						691mw					
(13)	3 295w		1 039m		840vs			558s		363mw	348m
(14) I.r.	3 280w		1 056m		840vs			558s		358mw	336m
Raman			1 049mw	876w			617w			359w	343s

their parent carbons. In (**10**) the methyl groups were refined as rigid bodies. In (**12**), because of the large number of atoms in the structure and the consequent number of associated variables it was not possible, due to computer limitations, to use the normal 'riding model' for the hydrogen atoms. Consequently the hydrogen atoms were fixed in idealised calculated positions. Refinement was by block-cascade full-matrix least-squares methods to give for (**10**), $R = 0.038$, $R' = 0.039$ [$w^{-1} = \sigma^2(F) + 0.000\,62\,F^2$]; for (**12**), $R = 0.038$, $R' = 0.040$ [$w^{-1} = \sigma^2(F) + 0.000\,59\,F^2$]; for (**15**), $R = 0.059$, $R' = 0.055$ [$w^{-1} = \sigma^2(F) + 0.000\,51\,F^2$] ($R = \Sigma[|F_o| - |F_c|]/\Sigma|F_o|$). The maximum residual electron density in the final ΔF maps was 0.8, 0.6, and 0.5 e $Å^{-3}$ for (**10**), (**12**), and (**15**) respectively. The mean and maximum shift/error ratios in the final refinement cycle were for (**10**), 0.05 and 0.30; for (**12**), 0.01 and 0.08; and for (**15**), 0.01 and 0.03. Computations were carried out on an Eclipse S140 computer using the SHELXTL program system[14] and published scattering factors.[15]

Results and Discussion

Silyl and tin reagents provide useful sources of sulphur–nitrogen fragments in the synthesis of heterocycles.[16,17] Usually the driving force for these reactions is the formation of a M–Cl (M = Si or Sn) bond. Thus, for example $(Me_3Si)_2N_2S$ reacts with $S_4N_4Cl_2$ to give S_5N_6 whilst $(Me_2SnS_2N_2)_2$ (**1**) reacts with COF_2 to give the five-membered ring $C(O)S_2N_2$. Analogously, reaction of readily prepared (**1**) with $[MCl_2(PR_3)_2]$ complexes should provide rational syntheses of complexes containing the disulphur dinitrido ligand with elimination of Me_2SnCl_2. We have performed this type of reaction for a number of platinum complexes using dichloromethane [in which (**1**) is reasonably soluble] as the solvent. Surprisingly, the overall reaction in equation (1) is observed. The formation of the $S_2N_2H^-$ ligand

$$[MCl_2(PR_3)_2] + (Me_2SnS_2N_2)_2 \xrightarrow{CH_2Cl_2} [M(S_2N_2H)(PR_3)_2][Me_2SnCl_3] \quad (1)$$

and the $Me_2SnCl_3^-$ anion probably occurs as a result of HCl in the dichloromethane. If the reaction is carried out in the presence of 1,8-diazabicyclo[5.4.0]undec-7-ene $[M(S_2N_2)(PR_3)_2]$ complexes[4] are obtained. Although we have been able to isolate some $Me_2SnCl_3^-$ salts they are generally difficult to crystallise and so the reaction was carried out in the presence of $[NH_4][PF_6]$ or, in some cases, $[NH_4][BF_4]$ which enabled the isolation of PF_6^- and BF_4^- salts. The analyses for the compounds obtained are shown in Table 1. The levels of counter ions included were established by ion chromatography and in one case a mixed PF_6^-–Cl^- system was obtained. The scale of the reactions was kept to a minimum because of the high cost of the Pt and Pd starting materials.

The formation of $[CoCl_2(dppoe)]$ from the reaction of $CoCl_2$ and dppe in acetone is somewhat surprising. The microanalytical data are in good agreement with this formulation and the i.r. spectrum reveals a strong band at 1 120 cm^{-3} which also indicates the presence of P=O. This complex reacts with (**1**) to give $[\{Co(S_2N_2H)_2\}(dppoe)]$ (**15**) (from *X*-ray crystallography), indicating the weak co-ordination of the dppoe ligand. The structure of (**15**) is discussed below.

The vibrational spectra of the complexes (Table 2) show the expected bands due to the phosphine and $S_2N_2H^-$ ligands. Three ν(NS) vibrations are observed {as is the case in previous $[M(S_2N_2H)_2]$ complexes[18]}, although in some of the complexes reported here the SN bands are obscured by absorptions of the phosphines. The similarity of the spectra suggests that all of the compounds are isostructural; however the high frequency and the presence of two ν(NH) bands in (**8**) is not readily interpreted.* A weak interaction between the PMe_3 group and the NH may be responsible, alternatively this compound may exist as two phases in the solid state. The Raman spectra [compounds (**7**) and (**14**)] are consistent with those previously reported.[18]

Phosphorus-31 and ^1H n.m.r. data are given in Table 3. The ^1H n.m.r. show the expected bands due to phosphines, with the alkyl-substituted compounds having readily discernible bands for protons on PR_3 *trans* to nitrogen or sulphur. The simplest spectra are for the PMe_3 case, (**8**), where both $^2J(^{31}P–^1H)$ and $^3J(^{195}Pt–^1H)$ couplings are seen. The signals due to hydrogens on the $S_2N_2H^-$ group were not directly observed and this is not surprising since they are expected to be coupled to both platinum and phosphorus as well as being broadened due to hydrogen bonding. In the $Me_2SnCl_3^-$ salts the satellites due to coupling to tin were not well resolved.

The ^{31}P n.m.r. data are quite characteristic; the spectra consist of AX doublets together with, in the case of the platinum compounds, satellites due to ^{195}Pt. The $^2J(P–P)$ couplings are normal. The two $^1J(Pt–P)$ couplings observed in each compound are different to each other and are significantly different to those in the analogous $S_2N_2^{2-}$ complexes. The higher field resonance (δ_A) which has larger ^1J values is assigned as being

* The microanalysis for (**8**) was quite poor (Table 1) and it is possible that the presence of two bands may be due to an impurity.

Table 3. N.m.r. data*

Compound	δ_A/p.p.m.	$^{31}P-\{^1H\}$ δ_X/p.p.m.	^1J_A/Hz	^1J_X/Hz	^2J(P–P)/Hz	$R = J_A/J_X$	^1H
(2)	6.02	14.50	3 354.5	2 712.4	22	1.237	7.3 (m)
(3)	5.21	12.89	3 432.6	2 683.1	22	1.279	7.3 (m)
(4)							7.28 (m, 30), 1.25 (s, 6)
(5)	−14.20	−1.95	3 276.4	2 646.5	24	1.238	7.45 (m, 20), 2.0 (m, 6)
(7)	−27.46	−16.15	3 239.7	2 595.2	24	1.248	7.48 (m, 5), 1.94 (d, 3), 1.88 (d, 3)
(8)	−39.24	−23.73	3 129.9	2 565.9	24	1.22	1.97 [d, ^2J(P–H) 10.72, ^3J(Pt–H) 27.14 Hz] 1.92 [d, ^2J(P–H) 10.72, ^3J(Pt–H) 33.26 Hz]
(9)	−1.08	8.88	3 161.6	2 563.4	24	1.23	2.1 (m, 4), 1.2 (t, 3), 1.0 (t, 3)
(10)	−0.46	11.42	3 176.3	2 548.8	24	1.246	2.23 (m, 12), 1.39 (s, 6), 1.29 (t, 9), 1.09 (t, 9)
(11)	−9.78	0.58	3 176.2	2 539.1	24	1.251	2.05 (m, 2), 1.55 (m, 2), 1.05 (t, 3)
(12)	−9.52	2.52	3 164.0	2 561.0	22	1.235	2.1 (m, 2), 1.5 (m, 4), 0.9 (m, 3)
(13)	38.63	44.56	3 161.6	2 734.4	9.8	1.156	7.6 (m, 10), 2.7 (m, 2)
(14)	55.41	60.76			24		7.6 (m, 10), 2.7 (m, 2)

* Resonances due to PF_6^- not listed.

Table 4. Selected bond distances (Å) and angles (°) in $[Pt(S_2N_2H)(PEt_3)_2][Me_2SnCl_3]$ (**10**)

Pt(1)–P(1)	2.306(4)	S(1)–N(1)	1.572(12)	Pt(1)–P(2)	2.263(3)	S(1)–N(2)	1.554(10)
Pt(1)–S(2)	2.281(4)	S(2)–N(2)	1.667(10)	Pt(1)–N(1)	2.041(9)	Sn(1)–Cl(1)	2.491(3)
P(1)–C(1)	1.803(14)	Sn(1)–Cl(2)	2.405(4)	P(1)–C(3)	1.806(7)	Sn(1)–Cl(3)	2.773(3)
P(1)–C(5)	1.826(12)	Sn(1)–C(13)	2.090(8)	P(2)–C(7)	1.808(3)	Sn(1)–C(14)	2.087(15)
P(2)–C(9)	1.845(4)			P(2)–C(11)	1.810(14)		
P(1)–Pt(1)–P(2)	97.9(1)	C(7)–P(2)–C(11)	104.4(4)	P(1)–Pt(1)–S(2)	171.3(1)	C(9)–P(2)–C(11)	104.1(5)
P(2)–Pt(1)–S(2)	90.8(1)	N(1)–S(1)–N(2)	109.4(5)	P(1)–Pt(1)–N(1)	87.0(3)	Pt(1)–S(2)–N(2)	105.2(4)
P(2)–Pt(1)–N(1)	174.9(3)	Pt(1)–N(1)–S(1)	121.2(6)	S(2)–Pt(1)–N(1)	84.3(3)	S(1)–N(2)–S(2)	119.8(7)
Pt(1)–P(1)–C(1)	122.0(5)	Cl(1)–Sn(1)–Cl(2)	96.3(1)	Pt(1)–P(1)–C(3)	110.6(4)	Cl(1)–Sn(1)–Cl(3)	170.3(1)
C(1)–P(1)–C(3)	102.4(8)	Cl(2)–Sn(1)–Cl(3)	93.4(1)	Pt(1)–P(1)–C(5)	110.7(5)	Cl(1)–Sn(1)–C(13)	93.0(4)
C(1)–P(1)–C(5)	105.7(7)	Cl(2)–Sn(1)–C(13)	99.1(3)	C(3)–P(1)–C(5)	103.7(4)	Cl(3)–Sn(1)–C(13)	86.1(3)
Pt(1)–P(2)–C(7)	113.7(1)	Cl(1)–Sn(1)–C(14)	92.7(4)	Pt(1)–P(2)–C(9)	115.8(2)	Cl(2)–Sn(1)–C(14)	99.9(4)
C(7)–P(2)–C(9)	105.6(2)	Cl(3)–Sn(1)–C(14)	85.0(3)	Pt(1)–P(2)–C(11)	112.2(4)	C(13)–Sn(1)–C(14)	159.5(5)

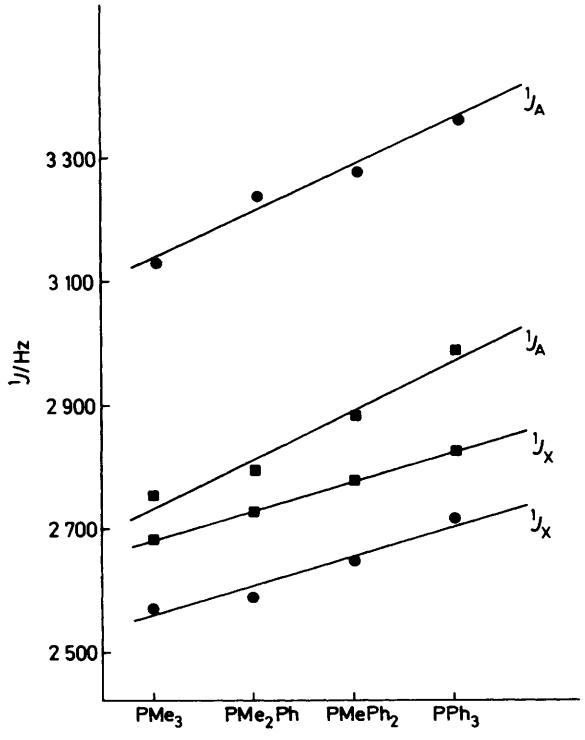

Figure 1. Variation of $^1J(^{195}Pt-^{31}P)$ in $[Pt(S_2N_2H)(PR_3)_2]^+$ (●) and $[Pt(S_2N_2)(PR_3)_2]$ (■) with the nature of PR_3

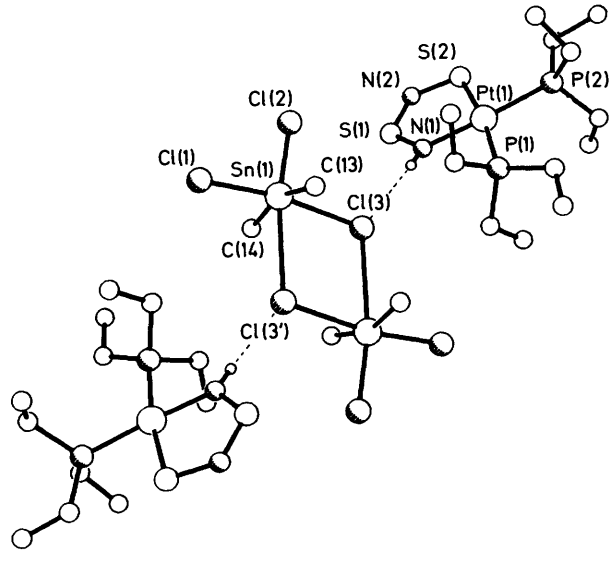

Figure 2. The *X*-ray structure of (**10**)

due to phosphorus *trans* to nitrogen for a number of reasons. Firstly, the Pt–P bond lengths in (**10**) and (**12**) are significantly shorter for P(2) *trans* to nitrogen. Second, ^{31}P spectra for (**8**) were obtained with various types of decoupling; under selective decoupling of the ^1H region due to the Me groups of the PMe_3 ligand the signals at δ_A were broadened relative to δ_X suggesting additional coupling as a result of the *trans* NH group. Further-

more, the magnitude of ^1J_A is increased by *ca.* 360 Hz whilst ^1J_X is reduced in magnitude by *ca.* 120 Hz on going from $S_2N_2^{2-}$ to $S_2N_2H^-$. This can be expressed as the ratio J_A/J_X which is *ca.* 1.05 and 1.2 respectively. The relationship is shown graphically in Figure 1 for PMe_3 through to PPh_3. It is to be expected that ^1J due to phosphorus *trans* to nitrogen would be more sensitive to protonation than the coupling at phosphorus *trans* to sulphur.

The compounds reported here are formally imines whilst the previously reported $S_2N_2^{2-}$ ligand may be regarded as an imido group. Several factors could affect the relative magnitude of the ^1J coupling constants for phosphorus *trans* to nitrogen. For example, simple σ-bonding/bond distance arguments suggest that ^1J would be expected to rise on going from imido to imine co-ordination if the imine is a poorer σ donor, resulting in the platinum being a better acceptor of electron density from the *trans* phosphine and thus having shorter Pt–P bond lengths for the imine complexes. This argument is not supported by the *X*-ray crystallographic studies which reveal essentially unchanged Pt–P distances on going from $[Pt(S_2N_2)(PPh_3)_2]$[19] to (**10**) and (**12**). Clearly, additional factors may be involved and we will reconsider this effect when more structural data are available.

Comparison of the ^{31}P chemical shift data for $[Pt(S_2N_2H)(PR_3)_2][PF_6]$, $[Pt(S_2N_2)(PR_3)_3]$, $[PtCl_2(PR_3)_2]$, and the

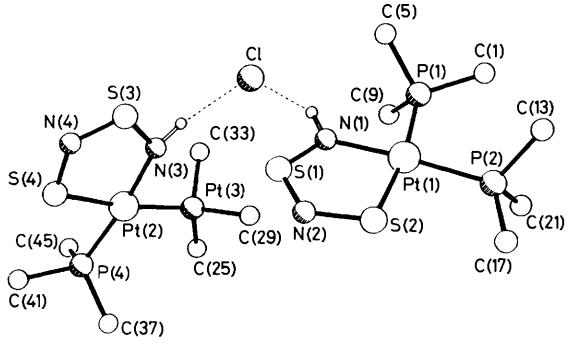

Figure 3. The *X*-ray structure of (**12**)

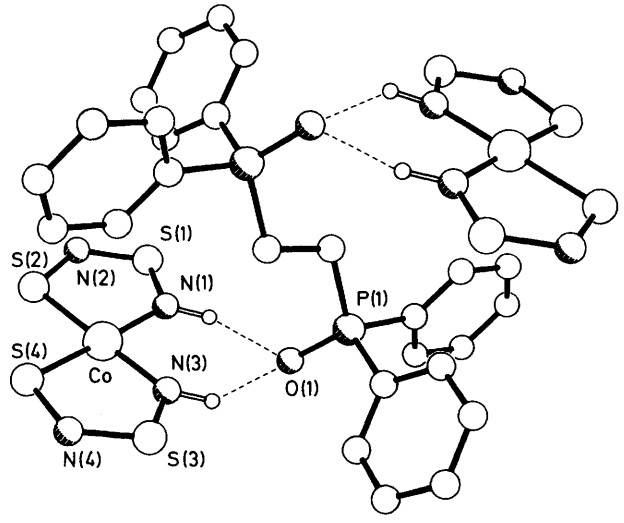

Figure 4. The *X*-ray structure of (**15**)

Table 5. Selected bond distances (Å) and angles (°) in $[Pt(S_2N_2H)(PBu^n_3)_2]_2[PF_6]Cl$ (**12**)

Pt(1)–S(2)	2.291(2)	Pt(2)–S(4)	2.277(2)	Pt(1)–P(1)	2.311(2)	Pt(2)–P(3)	2.318(2)
Pt(1)–P(2)	2.262(2)	Pt(2)–P(4)	2.273(2)	Pt(1)–N(1)	2.024(6)	Pt(2)–N(3)	2.034(6)
S(1)–N(1)	1.585(5)	S(3)–N(3)	1.590(7)	S(1)–N(2)	1.544(8)	S(3)–N(4)	1.543(7)
S(2)–N(2)	1.662(8)	S(4)–N(4)	1.650(7)	P(1)–C(1)	1.830(8)	P(3)–C(25)	1.820(8)
P(1)–C(5)	1.822(9)	P(3)–C(29)	1.829(9)	P(1)–C(9)	1.838(9)	P(3)–C(33)	1.825(9)
P(2)–C(13)	1.832(8)	P(4)–C(37)	1.808(10)	P(2)–C(17)	1.808(10)	P(4)–C(41)	1.841(9)
P(2)–C(21)	1.823(8)	P(4)–C(45)	1.853(10)				
S(2)–Pt(1)–P(1)	170.6(1)	S(4)–Pt(2)–P(4)	89.4(1)	S(2)–Pt(1)–P(2)	91.0(1)	S(4)–Pt(2)–P(3)	171.5(1)
P(1)–Pt(1)–P(2)	98.4(1)	S(4)–Pt(2)–N(3)	84.4(2)	S(2)–Pt(1)–N(1)	84.5(1)	P(3)–Pt(2)–P(4)	99.0(1)
P(1)–Pt(1)–N(1)	86.1(1)	P(4)–Pt(2)–N(3)	173.2(2)	P(2)–Pt(1)–N(1)	175.5(1)	P(3)–Pt(2)–N(3)	87.2(2)
N(1)–S(1)–N(2)	109.3(3)	Pt(2)–S(4)–N(4)	105.2(3)	Pt(1)–S(2)–N(2)	104.7(3)	N(3)–S(3)–N(4)	108.8(4)
Pt(1)–P(1)–C(1)	120.8(3)	Pt(2)–P(3)–C(29)	112.6(3)	Pt(1)–P(1)–C(5)	111.1(2)	Pt(2)–P(3)–C(25)	121.3(3)
C(1)–P(1)–C(5)	102.9(4)	Pt(2)–P(3)–C(33)	109.2(3)	Pt(1)–P(1)–C(9)	110.2(3)	C(25)–P(3)–C(29)	103.9(4)
C(1)–P(1)–C(9)	107.1(4)	C(29)–P(3)–C(33)	103.1(4)	C(5)–P(1)–C(9)	103.2(4)	C(25)–P(3)–C(33)	105.2(4)
Pt(1)–P(2)–C(13)	114.4(3)	Pt(2)–P(4)–C(41)	115.2(3)	Pt(1)–P(2)–C(17)	114.8(3)	Pt(2)–P(4)–C(37)	119.1(3)
C(13)–P(2)–C(17)	103.1(4)	Pt(2)–P(4)–C(45)	112.9(3)	Pt(1)–P(2)–C(21)	113.6(3)	C(37)–P(4)–C(41)	103.6(4)
C(13)–P(2)–C(21)	106.0(4)	C(41)–P(4)–C(45)	101.2(4)	C(17)–P(2)–C(21)	103.7(5)	C(37)–P(4)–C(45)	102.6(5)
Pt(1)–N(1)–S(1)	121.1(3)	S(3)–N(4)–S(4)	120.7(4)	S(1)–N(2)–S(2)	120.4(4)	Pt(2)–N(3)–S(3)	120.8(4)
						P(3)–C(25)–C(26)	117.4(6)

Table 6. Selected bond distances (Å) and angles (°) in $[\{Co(S_2N_2H)_2\}_2(dppoe)]$ (**15**)

Co–S(2)	2.125(3)	S(3)–N(4)	1.551(7)	Co–S(4)	2.118(2)	S(4)–N(4)	1.670(8)
Co–N(1)	1.863(6)	P(1)–O(1)	1.540(5)	Co–N(3)	1.858(8)	P(1)–C(1)	1.816(6)
S(1)–N(1)	1.595(7)	P(1)–C(7)	1.804(7)	S(1)–N(2)	1.526(8)	P(1)–C(13)	1.809(8)
S(2)–N(2)	1.674(7)			S(3)–N(3)	1.592(6)		
S(2)–Co–S(4)	92.7(1)	O(1)–P(1)–C(1)	112.0(3)	S(2)–Co–N(1)	87.6(2)	O(1)–P(1)–C(7)	110.9(3)
S(4)–Co–N(1)	176.5(2)	C(1)–P(1)–C(7)	105.1(3)	S(2)–Co–N(3)	179.5(2)	O(1)–P(1)–C(13)	114.0(3)
S(4)–Co–N(3)	87.8(2)	C(1)–P(1)–C(13)	106.1(3)	N(1)–Co–N(3)	91.9(3)	C(7)–P(1)–C(13)	108.1(3)
N(1)–S(1)–N(2)	106.6(4)	Co–N(1)–S(1)	122.5(4)	Co–S(2)–N(2)	105.4(3)	S(1)–N(2)–S(2)	118.0(5)
N(3)–S(3)–N(4)	107.0(4)	Co–N(3)–S(3)	122.3(4)	Co–S(4)–N(4)	106.2(2)	S(3)–N(4)–S(4)	116.5(4)

Table 7. Atomic co-ordinates for (**10**)

Atom	*x*	*y*	*z*	Atom	*x*	*y*	*z*
Pt(1)	5 160(1)	6 219(1)	1 288(1)	C(7)	6 401(1)	5 204(1)	2 606(1)
P(1)	6 341(2)	7 001(2)	1 339(1)	C(8)	5 917(7)	5 621(8)	3 015(5)
P(2)	5 812(2)	5 059(2)	1 767(1)	C(9)	6 550(1)	4 577(1)	1 366(1)
S(1)	3 489(2)	7 209(2)	669(2)	C(10)	6 133(10)	4 350(9)	673(3)
S(2)	3 880(2)	5 613(2)	1 155(1)	C(11)	5 078(9)	4 238(7)	1 795(6)
N(1)	4 476(7)	7 224(6)	870(4)	C(12)	5 486(10)	3 434(8)	2 111(8)
N(2)	3 182(7)	6 344(6)	827(5)	Sn(1)	4 136(1)	9 292(1)	−897(1)
C(1)	7 385(9)	6 593(10)	1 668(9)	Cl(1)	3 717(3)	9 704(3)	−2 065(1)
C(2)	8 108(12)	7 166(12)	1 702(11)	Cl(2)	3 385(3)	8 000(2)	−1 043(2)
C(3)	6 361(10)	7 332(2)	537(2)	Cl(3)	4 734(3)	9 092(2)	439(1)
C(4)	6 335(1)	6 655(1)	53(1)	C(13)	5 308(4)	8 859(7)	−942(6)
C(5)	6 311(9)	7 970(7)	1 773(5)	C(14)	3 239(9)	10 061(8)	−675(6)
C(6)	6 369(14)	7 878(10)	2 468(7)				

Table 8. Atomic co-ordinates for (**12**)

Atom	*x*	*y*	*z*	Atom	*x*	*y*	*z*
Pt(1)	13 313(1)	6 621(1)	5 301(1)	P(4)	14 519(2)	7 404(2)	382(1)
S(1)	14 350(2)	5 776(2)	3 975(1)	N(3)	13 368(6)	5 641(5)	2 230(3)
S(2)	15 156(2)	6 500(2)	4 947(1)	N(4)	14 675(6)	4 368(5)	1 690(4)
P(1)	11 445(2)	6 606(2)	5 515(1)	C(25)	12 511(7)	8 925(6)	1 388(4)
P(2)	13 502(2)	7 290(2)	6 195(1)	C(26)	11 586(9)	9 605(7)	1 679(5)
N(1)	13 269(3)	6 035(4)	4 472(3)	C(27)	11 401(11)	10 528(8)	1 214(7)
N(2)	15 336(5)	6 022(5)	4 243(3)	C(28A)	10 796(19)	10 414(16)	712(12)
C(1)	10 658(7)	6 878(6)	6 317(4)	C(28B)	10 521(30)	11 216(26)	1 368(19)
C(2)	9 426(7)	6 923(7)	6 384(5)	C(29)	12 908(7)	7 890(6)	2 666(4)
C(3)	8 808(9)	7 022(10)	7 081(7)	C(30)	14 016(7)	8 108(6)	2 702(4)
C(4A)	9 100(20)	6 348(17)	7 593(12)	C(31)	14 104(7)	8 422(6)	3 367(4)
C(4B)	9 243(32)	7 407(27)	7 560(20)	C(32)	15 251(10)	8 555(8)	3 424(6)
C(5)	11 060(6)	5 437(6)	5 466(4)	C(33)	11 304(7)	7 327(7)	2 021(4)
C(6)	11 552(7)	4 615(6)	5 934(5)	C(34)	10 889(8)	7 154(9)	1 404(5)
C(7)	11 313(8)	3 667(7)	5 808(6)	C(35)	9 812(10)	6 774(12)	1 547(6)
C(8)	11 735(10)	2 866(8)	6 254(8)	C(36)	9 357(12)	6 647(17)	962(10)
C(9)	10 829(7)	7 388(6)	4 845(4)	C(37)	15 104(8)	8 498(6)	371(5)
C(10)	11 143(8)	8 395(6)	4 706(5)	C(38)	15 832(9)	8 435(7)	857(5)
C(11)	10 603(8)	8 982(7)	4 135(5)	C(39)	16 510(11)	9 332(8)	741(7)
C(12)	10 951(10)	9 963(8)	3 940(6)	C(40)	17 294(15)	9 267(12)	1 184(11)
C(13)	13 074(7)	6 581(6)	7 013(4)	C(41)	15 549(8)	6 746(6)	−179(4)
C(14)	13 416(7)	5 533(6)	7 033(4)	C(42)	16 678(8)	6 604(7)	−58(5)
C(15)	12 927(8)	4 928(7)	7 661(5)	C(43)	17 404(9)	5 969(9)	−540(7)
C(16)	13 294(10)	3 880(8)	7 679(6)	C(44)	18 550(12)	5 839(12)	−458(9)
C(17)	14 882(7)	7 487(7)	6 232(5)	C(45)	13 454(8)	7 795(7)	−152(4)
C(18)	15 329(8)	8 323(7)	5 728(5)	C(46)	12 983(9)	7 005(8)	−353(5)
C(19)	16 600(10)	8 253(11)	5 662(6)	C(47)	12 073(12)	7 412(11)	−796(8)
C(20)	16 998(14)	9 102(15)	5 172(8)	C(48)	11 654(13)	6 784(15)	−1 040(9)
C(21)	12 755(7)	8 465(6)	6 225(5)	P(5)	15 819(2)	8 752(2)	7 905(1)
C(22)	12 661(9)	8 902(8)	6 865(5)	F(1)	15 194(8)	9 213(7)	7 361(5)
C(23)	12 021(13)	9 867(9)	6 832(7)	F(2)	16 493(9)	8 220(7)	8 415(5)
C(24)	11 717(17)	10 257(14)	7 389(9)	F(3)	16 830(7)	9 225(6)	7 540(4)
Pt(2)	13 886(1)	6 547(1)	1 386(1)	F(4)	15 596(10)	9 575(8)	8 257(7)
S(3)	13 812(2)	4 543(2)	2 309(1)	F(5)	14 807(7)	8 279(6)	8 296(5)
S(4)	14 960(2)	5 243(2)	1 071(1)	F(6)	16 080(7)	7 869(6)	7 557(5)
P(3)	12 667(2)	7 719(2)	1 840(1)	Cl	11 744(2)	5 489(2)	3 581(1)

parent phosphines reveals consistent relative shifts; mean values (p.p.m.) are given below.

$$\delta[(S_2N_2H)\text{ complex}] - \delta[\text{free phosphine}] = \begin{matrix} 19 \text{ for } \delta_A \\ 29 \text{ for } \delta_X \end{matrix}$$

$$\delta[(S_2N_2H)\text{ complex}] - \delta[\textit{cis}\text{-}PtCl_2(PR_3)_2] = \begin{matrix} -11\ \delta_A \\ 0\ \ \delta_X \end{matrix}$$

$$\delta[(S_2N_2H)\text{ complex}] - \delta[(S_2N_2)\text{ complex}] = \begin{matrix} -3\ \delta_A \\ -8\ \delta_X \end{matrix}$$

The *X*-ray structures of (**10**), (**12**), and (**15**) (Tables 4—10, Figures 2—5) reveal a number of interesting features. The MS_2N_2 rings are in all cases essentially planar with square-planar co-ordination of the metal. In (**10**) the maximum deviations from the mean plane of the MS_2N_2 ring are (within the ring) 0.01 Å for N(1) and (in the co-ordination sphere) 0.09 Å for P(2). Interestingly, in (**12**) one cation is more distorted from planar than the other with the maximum deviations being 0.006 [N(1)] and 0.045 Å [P(2)] in one molecule and 0.020 [N(3)] and 0.16 Å [P(4)] in the other. In (**15**) the maximum deviation from the plane for the whole of the cobalt complex is

Table 9. Atomic co-ordinates for (**15**)

Atom	*x*	*y*	*z*	Atom	*x*	*y*	*z*
Co	1 856(1)	3 613(1)	1 003(1)	C(2)	−3 780(7)	1 526(8)	−364(6)
S(1)	379(2)	4 183(2)	−1 017(2)	C(3)	−4 959(8)	1 441(10)	−906(7)
S(2)	2 600(2)	4 685(3)	153(2)	C(4)	−5 355(7)	410(11)	−1 451(7)
S(3)	1 923(2)	2 229(2)	2 773(2)	C(5)	−4 605(7)	−505(9)	−1 477(6)
S(4)	3 431(2)	3 613(3)	2 160(2)	C(6)	−3 431(6)	−421(7)	−944(5)
P(1)	−1 518(2)	731(2)	351(1)	C(7)	−1 434(5)	−102(7)	1 414(5)
O(1)	−1 155(4)	2 073(4)	578(3)	C(8)	−1 168(6)	539(8)	2 259(5)
N(1)	498(6)	3 524(6)	−37(4)	C(9)	−1 167(8)	−50(11)	3 071(6)
N(2)	1 550(7)	4 807(7)	−896(5)	C(10)	−1 446(8)	−1 261(12)	3 056(7)
N(3)	1 194(6)	2 675(6)	1 736(4)	C(11)	−1 690(7)	−1 908(9)	2 228(7)
N(4)	3 177(6)	2 758(7)	2 999(4)	C(12)	−1 699(6)	−1 322(7)	1 398(5)
C(1)	−3 033(6)	591(7)	−396(5)	C(13)	−657(5)	−76(7)	−253(5)

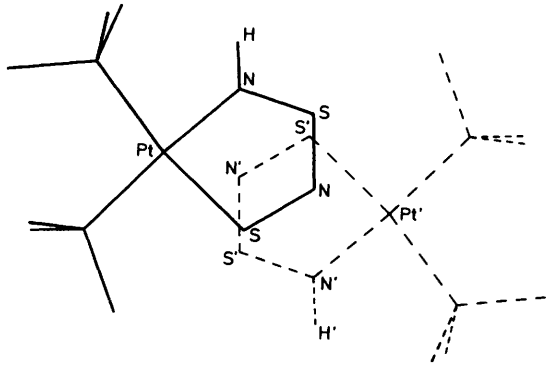

Figure 5. View perpendicular to the MS_2N_2 mean plane in (**12**) showing the overlap of the rings in the cations

0.06 Å for N(4). In the cobalt case the planarity of complexes of this type has previously only been deduced from vibrational spectroscopy [18] and some workers [20] have claimed that the i.r. spectrum of $Co(S_2N_2H)_2$ indicates deviation from planar geometry.

The bond distances and angles within the $S_2N_2H^-$ ligands appear to be insensitive to the nature of *trans* ligand on the metal. It is difficult to establish bond orders for sulphur–nitrogen bonds but it is clear (Table 10) that N(2)–S(2) is close to a single bond whilst the other two bonds do involve some π-delocalisation. The S(1)–N(2) distance is significantly shorter than the S(1)–N(1) distance which appears to be intermediate in character between a single and a double bond. The angles within the five-membered MS_2N_2 rings support this view with both nitrogens being trigonal (sp^2 hybridised), S(1) being essentially tetrahedral whilst S(2) has noticeably smaller values.

In all three structures the positions of the imine hydrogen atoms in the $S_2N_2H^-$ ligands were located from difference maps. Hydrogen-bonding interactions are important and provide additional confirmatory evidence as to the locations of the protons. In (**10**) (Figure 3) the bridging chlorine atom of the dimeric $(Me_2SnCl_3)_2^{2-}$ anion bonds to the imine ligand proton [N ··· Cl 3.22, H ··· Cl 2.41 Å, N–H(1)N–Cl 142°]. The anion in (**10**) is best regarded as a loosely associated dimer and not a monomeric five-co-ordinate tin species as has been proposed by some previous workers.[21,22] The bridging Sn–Cl distances are Sn–Cl(3) 2.773(3) and Sn–Cl(3′) 3.205(3) Å, the two halves of the dimer being related by a crystallographic centre of symmetry. In (**12**) there are two types of anion (PF_6^-, Cl^-) and two crystallographically independent cations. The chloride anion bridges the two independent cations [H(1) ··· Cl 2.23, H(3)N ··· Cl 2.21, N(1) ··· Cl 3.12, N(3) ··· Cl 3.12 Å, N(1)–H(1)N–Cl 153, N(3)–H(3)–Cl 158, H(1)N–Cl–H(3)N 112°, Figure 3] whilst the PF_6^- is not involved in any interactions. In (**15**) (Figure 4) the *cis* NH groups interact with the P=O group [H(1)N ··· O(1) 2.07, H(3)N ··· O(1) 1.98, N(1) ··· O(1) 2.92, N(3) ··· O(1) 2.88 Å, N(1)–H(1)–O(1) 165, N(3)–H(3)N–O(3) 141°].

Table 10. Comparison of distances and angles in the MS_2N_2 ring for (**10**), (**12**), (**15**), and $[Pt(S_2N_2H)(PMe_2Ph)_2][BF_4]$ (**16**) (ref. 8)

Bond length (Å) or angle (°)	Compound (**10**)	(**12**)	(**15**)	(**16**)
M–P(1)	2.306(4)	2.311(2) 2.318(2)		2.303(2)
M–P(2)	2.263(3)	2.262(2) 2.273(2)		2.261(2)
M–N(1)	2.041(9)	2.024(6) 2.034(6)	1.863(6)	2.015(7)
M–S(2)	2.281(4)	2.291(2) 2.277(2)	2.125(3)	2.283(2)
N(1)–S(1)	1.572(12)	1.585(5) 1.590(7)	1.595(7)	1.595(7)
S(1)–N(2)	1.554(10)	1.544(8) 1.543(7)	1.526(8)	1.538(9)
N(2)–S(2)	1.667(10)	1.662(8) 1.650(7)	1.674(7)	1.649(8)
N(1)–M–S(2)	84.3(3)	84.5(1) 84.4(2)	87.6(2)	84.6(2)
M–N(1)–S(1)	121.2(6)	121.1(3) 120.8(4)	122.5(4)	121.4(4)
N(1)–S(1)–N(2)	109.4(5)	109.3(3) 108.8(4)	106.6(4)	108.1(4)
S(1)–N(2)–S(2)	119.8(7)	120.4(4) 120.7(4)	118.0(5)	121.6(5)
N(2)–S(2)–M	105.2(4)	104.7(3) 105.2(3)	105.4(3)	104.4(3)

Table 11. Stacking properties and distances (Å) established from *X*-ray crystallography

Compound	Type of stacking	Interplanar separation[a]	Nearest contact
(**8**)	Continuous	3.8[b]	3.9 [Pt ··· S(1′)]
(**16**)	Infinite	3.5	3.62 [Pt ··· S(1′)]
	'dimers'	4.6	5.04 [Pt ··· S(1″)]
			4.70 [Pt ··· N(2″)]
(**12**)	Loose isolated 'dimers' for half of cations	3.6	3.66 [S(1) ··· S(2′)]
(**10**)	None		
(**15**)	None		

[a] Refers to MS_2N_2 means planes, unless stated otherwise. [b] Refers to mean plane of co-ordination shell.

As mentioned above, some of the structures of these types of complexes consist of columns of cations and anions with the MS_2N_2 rings in the cations overlying each other.[8] Clearly, changes in the bulk of the phosphine and the nature of the cation would be expected to affect the stacking. The inter-cation separations of a number of compounds are summarised in Table 11. In (**10**) the large tin anion prevents any close interactions between cations. In (**12**), which contains the relatively bulky PBu^n_3 group, only one of the two crystallographically independent cations forms an overlapping MS_2N_2 dimer pair (Figure 5). From Table 11 it appears that although only a few structures are currently available, increasing the size of the phosphine or the anion affects the interplanar separation of the cations and further studies into this effect are underway.

Acknowledgements

We are grateful to Johnson Matthey for loans of precious metal salts and to Erica Parkes for measuring the Raman spectra.

References

1 J. Weiss, *Fortschr. Chem. Forsch.*, 1966, **5**, 635.
2 J. D. Woollins, R. Grinter, M. K. Johnson, and A. J. Thomson, *J. Chem. Soc., Dalton Trans.*, 1980, 1910.
3 P. F. Kelly and J. D. Woollins, *Polyhedron*, 1986, **5**, 607.
4 P. Bates, M. B. Hursthouse, P. F. Kelly, and J. D. Woollins, *J. Chem. Soc., Dalton Trans.*, 1986, 2367.
5 J. D. Woollins, *Polyhedron*, 1984, **3**, 1365.
6 N. P. C. Walker, M. B. Hursthouse, C. P. Warrens, and J. D. Woollins, *J. Chem. Soc., Chem. Commun.*, 1985, 227.
7 H. W. Roesky and H. Weizer, *Angew. Chem., Int. Ed. Engl.*, 1973, **12**, 674.
8 R. Jones, P. F. Kelly, C. P. Warrens, D. J. Williams, and J. D. Woollins, *J. Chem. Soc., Chem Commun.*, 1986, 711.
9 G. Booth and J. Chatt, *J. Chem. Soc. A*, 1966, 834.
10 F. R. Hartley, 'The Chemistry of Platinum and Palladium,' Applied Science, London, 1973.
11 J. C. Bailar, jun., and H. Itatani, *Inorg. Chem.*, 1965, **4**, 1618.
12 M. C. Clark and L. E. Manzer, *J. Organomet. Chem.*, 1973, **59**, 411.
13 W. Dew-Horrocks, jun., G. R. VanHecke, and D. Dew-Hall, *Inorg. Chem.*, 1967, **6**, 694.
14 G. M. Sheldrick, SHELXTL, An integrated system for solving, refining and displaying crystal structures from diffraction data, University of Göttingen, Federal Republic of Germany, 1978; Revision 4.1, 1983.
15 'International Tables for *X*-Ray Crystallography,' Kynoch Press, Birmingham, 1974, vol. 4, pp. 99—149.
16 H. G. Heal, 'The Inorganic Heterocyclic Chemistry of Sulphur, Nitrogen and Phosphorus,' Academic Press, London, 1980.
17 H. W. Roesky, M. N. S. Rao, T. Nakajima, and W. S. Sheldrick, *Chem. Ber.*, 1979, **112**, 3531.
18 D. B. Powell and J. D. Woollins, *Spectrochim. Acta, Part A*, 1980, **36**, 447.
19 R. Jones, P. F. Kelly, D. J. Williams, and J. D. Woollins, *Polyhedron*, 1985, **4**, 1947.
20 D. T. Haworth, G. Yu. Lin, D. Brown, and J. Chen, *Spectrochim. Acta, Part A*, 1978, **34**, 371.
21 A. J. Butienshaw, M. Duchene, and M. Webster, *J. Chem. Soc., Dalton Trans.*, 1975, 2230.
22 F. W. B. Einstein and B. R. Penfold, *J. Chem. Soc. A*, 1968, 3019.

Received 19*th May* 1986; *Paper* 6/966